PHYSICAL REVIEW C VOLUME 44, NUMBER 2 AUGUST 1991

Antiproton-induced elastic and inelastic scattering at intermediate energies

W.-H. Ma* and D. Strottman
Theoretical Division, Los Alamos National Laboratory, Los Alamos, New Mexico 87545
(Received 8 March 1991)

Results are presented of zero-parameter calculations of antiproton-induced elastic and inelastic scattering from ^{12}C, ^{16}O, and ^{40}Ca for five kinetic energies from 0.23 to 1.83 GeV. The Glauber model is employed with microscopic shell-model wave functions, Woods-Saxon single-particle wave functions, and experimental $\bar{p}N$ amplitudes.

I. INTRODUCTION

With the construction and subsequent operation of the Low Energy Antiproton Ring (LEAR), beams of low-energy anitprotons with previously unobtainable intensity and quality were possible. Elastic- and inelastic-scattering experiments were performed on several nuclei in both the p and sd shell [1–5] as well as on targets of heavier mass. In the very near future experiments with antiprotons having momentum of up to 2 GeV/c will be possible. It is the purpose of this article to report results of initial calculations of $\bar{p}$-nucleus scattering for energies that span this new energy region and for which the elementary $\bar{p}N$ amplitudes are known.

The Glauber model [6] has proven capable of providing an excellent description of the low-energy $\bar{p}$-nucleus scattering [7, 8]. Unlike the case for proton-nucleus scattering, the Glauber model appears to provide a reasonably accurate description of antiproton-nucleus scattering even at 47.9 MeV [9]. The results from Glauber model calculations at 180 MeV agree astonishingly well with experiment [9, 10]. A plausible reason for the validity of the Glauber model for antiproton scattering even at low energies is the presence of several partial waves that contribute to the reaction already at low energies, thus producing a very forward-peaked cross section near threshold. This earlier work using the Glauber model has been summarized at the 1988 PANIC meeting by Dalkarov and Karmonov [9]. Subsequently, the Glauber model was used to study the effects of annihilation and spin-flip on $\bar{p}$-nucleus reactions [11–13].

In this work we shall use the Glauber model which is not only quite accurate, but requires a minimum of input data for the calculations. This is essential when no $\bar{p}$-nucleus reaction data exist. Only the $\bar{p}N$ elementary amplitude – which is characterized by the total $\bar{p}N$ cross section and the ratio of the real-to-imaginary $\bar{p}N$ forward amplitude, the value of the diffraction-slope parameter – is required. These have been measured by Kaseno *et al.* [14] at 700 MeV/c and at several energies above 700 MeV/c by Jenni *et al.* [15]. Our version of the Glauber model uses microscopic wave functions determined from shell-model calculations. With the use of the experimentally determined $\bar{p}N$ interaction, we produce a zero-parameter calculation of elastic and inelastic scattering that includes both Pauli correlations and nucleon-nucleon correlations that are included via the shell model.

II. THE GLAUBER MODEL AND MICROSCOPIC WAVE FUNCTIONS

The details of our approach have been discussed in prior publications [16, 17] so we shall only summarize the method here. The shell model has been found over the past 40 years to be able to successfully predict and correlate large amounts of nuclear structure information. Our philosophy is to make use of this detailed information available from shell-model wave functions. Although Franco and Glauber had already applied the Glauber model to proton-deuteron scattering [18], the Glauber model was apparently first applied to hadron scattering on complex nuclei using (albeit extremely simple) microscopic wave functions by Bassel and Wilkins [19]. Our model extends this early work on using the Glauber model to describe hadron-nucleus reactions by using more sophisticated nuclear wave functions described by a series of Slater determinants-thereby including Pauli correlations-and by employing realistic single-particle wave functions.

The amplitude for $(\bar{p},\bar{p}')$ on a nucleus of A nucleons in the Glauber model may be written as

$$F_{M_f M_i}(q) = \frac{ik}{2\pi} \int d^2b\, e^{i\mathbf{q}\cdot\mathbf{b}} \left\langle J_f T_f M_f \left| 1 - \prod_j^A (1-\Gamma_j) \right| J_i T_i M_i \right\rangle , \tag{1}$$

where $\mathbf{b}$ is the impact parameter, k the incident pion momentum, $\mathbf{q} = \mathbf{k} - \mathbf{k}'$ is the momentum transfer, and Γ_j is the single-particle profile function

$$\Gamma_j(\mathbf{b}-\mathbf{s_j}) = \frac{1}{2\pi\, ik} \int d^2q\, f^{(N)}(q)\, e^{-i\mathbf{q}\cdot(\mathbf{b}-\mathbf{s_j})} \tag{2}$$

in which $\mathbf{s_j}$ is the projection of the vector position of a bound nucleon on the impact-parameter plane. The variables k and q in Eq. (1) are the laboratory variables while those in Eq. (2) refer to the $\bar{p}N$ center-of-mass system.

Equation (1) may be rewritten as

$$F_{M_f M_i}(q^2) = ike^{i\Delta M\pi/2}\int_0^\infty b\,db\,J_{\Delta M}(qb)\,\Gamma_{M_f M_i}(b), \tag{3}$$

where

$$\Gamma_{M_f M_i}(b)e^{i\Delta M\phi_b} = \left\langle J_f T_f M_f \left| 1-\prod_j^A(1-\Gamma_j)\right| J_i T_i M_i\right\rangle .$$

In Eq. (3), $\Delta M = M_i - M_f$, ϕ_b is the azimuthal angle of $\mathbf{b}$, and $\Gamma_{M_f M_i}(b)$ is the nuclear profile function resulting from evaluating the nuclear matrix element. The angular distribution is calculated by averaging over initial and summing over final states:

$$\frac{d\sigma}{d\Omega} = \frac{1}{2J_i+1}\sum_{M_i,M_f}|F_{M_f M_i}(q^2)|^2. \tag{4}$$

The single-particle profile function of Eq. (2) is obtained from the $\bar{p}N$ elementary amplitudes, $f^{(N)}(q)$, which are assumed to have a Gaussian form

$$f^{(N)} = \frac{ik\sigma^{(N)}(1-i\rho^{(N)})}{4\pi}e^{-\frac{1}{2}\beta^2q^2}\,, \quad N=n,p\,. \tag{5}$$

The values for σ, the total $\bar{p}N$ cross section, ρ, the ratio of the real-to-imaginary $\bar{p}N$ forward amplitude, and β the value of the diffraction-slope parameter, are taken from the experimental evaluations of Kaseno *et al.* [14] and of Jenn *et al.* [15]. We have assumed the $\bar{p}$-neutron and $\bar{p}$-proton interactions are the same. At the higher energies considered in this paper, one may expect the effect of the Coulomb interaction to be small and we omit it from the calculations. Its effect will be primarily to increase the cross section at small angles ($\theta < 5°$) and to make the minima less deep.

The initial and final nuclear wave functions that enter Eq. (1) were calculated as a sum of Slater determinants using a version of the Glasgow shell-model code [20]. The nuclei ^{16}O and ^{40}Ca are treated as closed-shell nuclei for which there is a single determinant; ^{12}C is treated within the complete p-shell basis for which there are 51 determinants. The wave functions for mass twelve were obtained using the matrix elements of Cohen and Kurath [21]. Because the wave functions are expressed in terms of Slater determinants, the many-body matrix elements of the Glauber operator, Eq. (3), may be expressed as the sum of $A \times A$ determinants. No problems of time-ordering occur. Our method of evaluating the scattering amplitude has the virtue that the effects of antisymmetry, or Pauli correlations, are explicitly included. No free parameters enter into the calculation.

The single-particle wave functions were calculated assuming a Woods-Saxon central potential and binding the nucleons at their experimental energies. The single-particle functions were then expanded in terms of three-dimensional Hermite polynomials for which the matrix elements of the profile function are easily calculated. The matrix elements of the profile functions were evaluated as described in Refs. [16] and [17]. Analytic expressions have been obtained for the single-particle profile function in the case of harmonic-oscillator functions [22]. However, in the case of using an effective charge $\beta \neq 1$, the quadrupole component of the matrix element of the single-particle profile function is enhanced by a factor of β and the integral is performed numerically.

III. RESULTS

The values of the total $\bar{p}N$ cross section σ, the ratio of the real-to-imaginary $\bar{p}N$ forward amplitude ρ, and the value of the diffraction-slope parameter β used in our calculations are given in Table 1. One may expect the $\bar{p}N$ interaction to be renormalized inside the nucleus. In Ref. [10] it was found that a better reproduction of 180 MeV $\bar{p}$ scattering data could be achieved by increasing the magnitude of σ by about 5 to 10%. There is a precedent for this: in studying pion- and kaon-induced reactions, Mizoguchi and Toki [23] found a similar effect. However, we shall not in this paper take this into account; if experience at lower energies is a guide, our calculations will be slightly lower than experiment.

The experimental values have uncertainties of a few percent. The calculated results are essentially independent of small variations in the value of β. Changing ρ will essentially only affect the depth of the minima which should not be expected to be accurately reproduced in our calculations since we have omitted the Coulomb interaction. Thus, the only essential sensitivity will be due to σ. The errors on this quantity are relatively small. The principal unknowns are the values of the three parameters for the $\bar{p}n$ interaction; we have taken them to be equal to the $\bar{p}p$ interaction, an approximation that has worked quite well at lower energies.

In Figs. 1–3 are shown results for elastic scattering of antiprotons on ^{12}C, ^{16}O, and ^{40}Ca for five kinetic energies from 0.23 to 1.83 GeV. The forward-angle cross section increases as one increases both the target mass and the incident energy. The maximum energy of antipro-

TABLE I. The values of the total $\bar{p}N$ cross section σ, the ratio of the real-to-imaginary $\bar{p}N$ forward amplitude ρ, and the value of the diffraction-slope parameter β used in the calculations. The values for 799 MeV/c are from Kaseno *et al.* [14]; the parameters for the remaining four energies are from Jenni *et al.* [15].

p (GeV/c)	T (GeV)	σ (fm^{-2})	ρ	β (GeV^{-2})
0.799	0.232	13.2	0.26	15.9
1.174	0.565	10.6	0.22	14.9
1.412	0.757	10.0	0.24	14.2
1.776	1.070	9.2	0.14	13.2
2.607	1.833	8.1	0.04	13.1

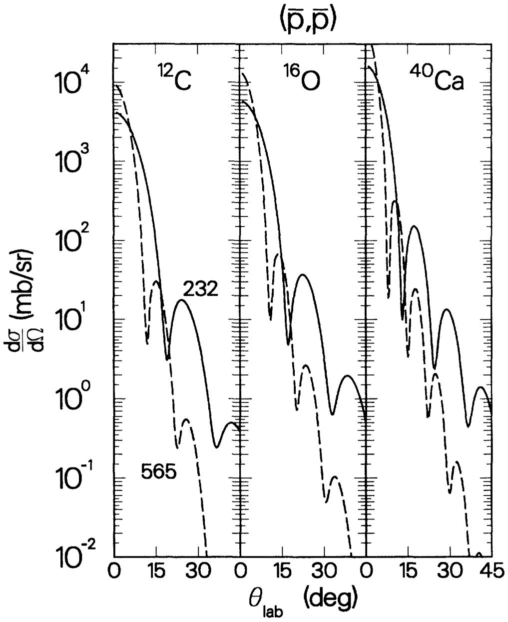

FIG. 1. Differential cross section in laboratory system for $\bar{p}$-elastic scattering on ^{12}C, ^{16}O, and ^{40}Ca. The solid lines are results for 232 MeV and the dashed lines for 565 MeV.

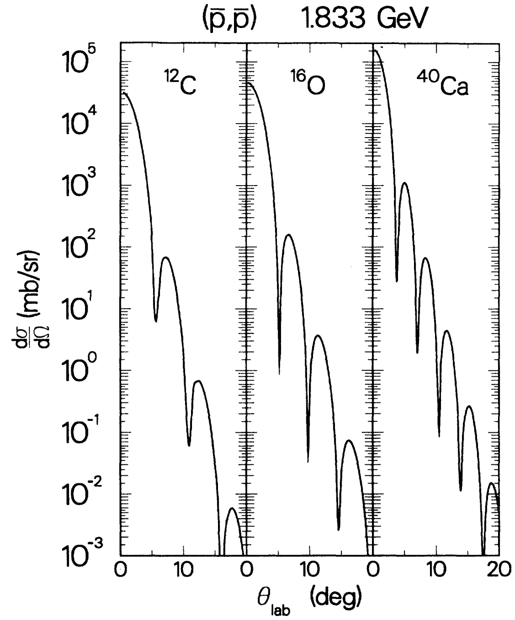

FIG. 3. Differential cross section in laboratory system for 1.83 GeV $\bar{p}$-elastic scattering on ^{12}C, ^{16}O, and ^{40}Ca.

tons with the upgraded LEAR should be intermediate between 1.07 and 1.83 GeV. Thus, even at the maximum energies, one should anticipate being able to measure the angular distribution for scattering from ^{12}C and ^{16}O out to the second minimum and perhaps the subsequent maximum. However, it will occur at the highest energies inside 20°. For ^{40}Ca one conceivably could measure past the third minima. It is in this region that effects due to the single-particle wave function and the value of the diffraction-slope parameter $\beta_{\bar{p}n}$ of the $\bar{p}n$ interaction will become more pronounced. Measurement of the angular distributions for ^{16,18}O or several of the Ca isotopes should allow one to more reliably extract the $\bar{p}n$ interaction from experiment.

In Fig. 4 are shown results at the five energies of in-

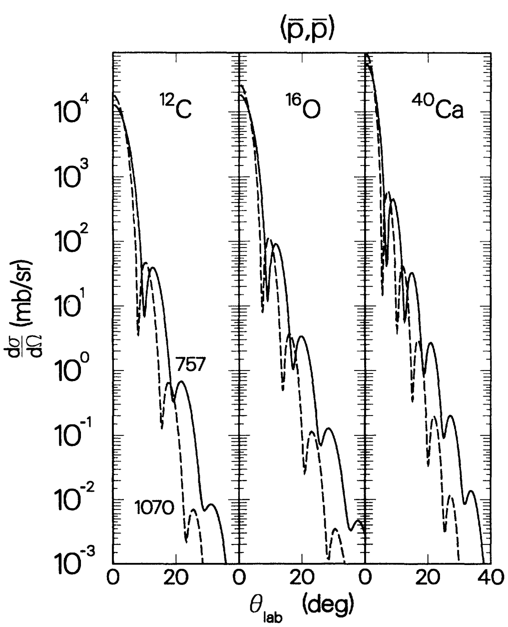

FIG. 2. Differential cross section in laboratory system for $\bar{p}$-elastic scattering on ^{12}C, ^{16}O, and ^{40}Ca. The solid lines are results for 757 MeV and the dashed lines for 1070 MeV.

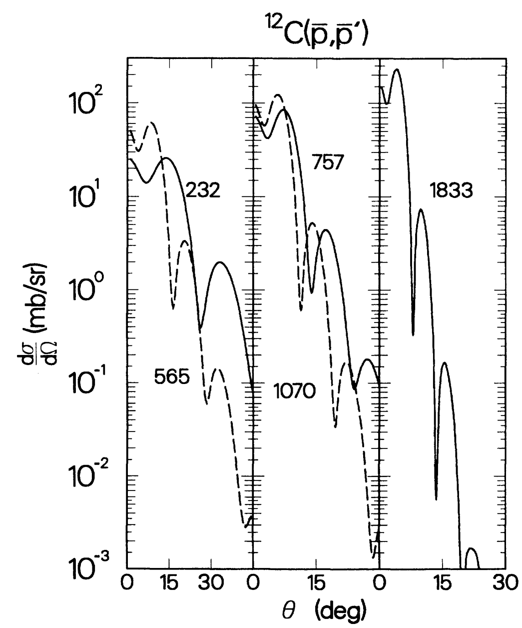

FIG. 4. Differential cross section in laboratory system for $\bar{p}$-inelastic scattering to the 2^+ of ^{12}C at five energies. Note that the 232 and 565 MeV curves extend to 45° whereas the remaining curves extend only to 30°. An effective charge of β=1.5 was used.

elastic excitation of the 2^+ of ^{12}C. Although the complete p-shell basis was used in the calculation, it is known from electromagnetic excitations that one must use an effective charge in order to reproduce the strength of the $2^+ \rightarrow 0^+$ transition. A similar result applies to both pion- [24] and $\bar{p}$-induced transitions [10]. We have used an effective charge of β=1.5, a value consistent with electromagnetic transitions and other hadron-induced reactions. A value of β=1 would have resulted in angular distributions of essentially identical shape but having a magnitude of approximately two smaller. We emphasize that unlike earlier work, our approach includes one-body through A-body scattering (always with the eikonal restriction that no nucleon is struck more than once). The $\bar{p}$ strongly interacts with the nucleus and a single-scattering approximation could be quite inaccurate.

Although no experimental data are now available for comparison with the theoretical predictions in this paper, the present results are sufficiently reliable to be a guide for measurements in the very near future. We believe that antiproton-induced elastic and inelastic scattering on nuclei at intermediate energies are particularly interesting. Some new and possibly unexpected phenomena may occur owing to the unique features of the many-body system. It may also produce new information on both the nuclear structure and the antinucleon-nucleon interaction, in particular the $\bar{p}$-neutron interaction.

ACKNOWLEDGMENTS

This work was performed under the auspices of the Division of Nuclear Physics, Office of High Energy and Nuclear Physics, U.S. Department of Energy. W-H.M. would like to thank the hospitality of the Nuclear Theory and Applications Group at Los Alamos National Laboratory.

---

* Permanent address: Institute of High Energy Physics (IHEP), Academia Sinica, Beijing, People's Republic of China.

[1] D. Garreta *et al.*, Phys. Lett. **135B**, 266 (1984); **139B**, 464 (1984).
[2] D. Garreta *et al.*, Phys. Lett. **149B**, 64 (1984); **151B**, 473 (1985).
[3] V. Ashford *et al.*, Phys. Rev. C **30**, 1080 (1984).
[4] W. Brückner *et al.*, Phys. Lett. **158B**, 180 (1985).
[5] M.-C. Lemaire *et al.*, Nucl. Phys. **A456**, 557 (1986).
[6] R. J. Glauber, *Lectures in Theoretical Physics* (Interscience, New York, 1959), Vol. 1, pp. 315–414.
[7] O. D. Dalkarov and V. A. Karmonov, Phys. Lett. **147B**, 1 (1984).
[8] O. D. Dalkarov and V. A. Karmonov, Nucl. Phys. **A478**, 635c (1988).
[9] O. D. Dalkarov, V. A. Karmonov, and A. V. Trukhov, Yad. Fiz. **45**, 688 (1987) [Sov. J. Nucl. Phys. **45**, 430 (1987)].
[10] W.-H. Ma and D. Strottman (unpublished).
[11] Z.-Q. Tan and Y.-T. Gu, J. Phys. G **15**, 1699 (1989).
[12] Z.-Q. Tan and W.-H. Ma, Nuovo Cimento **103A**, 185 (1990).
[13] Z.-Q. Tan, W.-H. Ma, and Y.-T. Gu, Nuovo Cimento **103A**, 1347 (1990).
[14] H. Kaseno *et al.*, Phys. Lett. **61B**, 203 (1976); **68B**, 487 (1977).
[15] P. Jenni *et al.*, Nucl. Phys. **B94**, 1 (1975).
[16] E. Oset and D. Strottman, Nucl. Phys. **A355**, 437 (1981); **A377**, 297 (1982).
[17] E. Oset and D. Strottman, Phys. Rev. C **42**, 2454 (1990).
[18] V. Franco and R.J. Glauber, Phys. Rev. **142**, 1195 (1966).
[19] R. H. Bassel and C. Wilkin, Phys. Rev. **174**, 1179 (1968).
[20] R. Whitehead, Nucl. Phys. **A182**, 290 (1972); R. R. Whitehead, A. Watt, B. J. Cole, and I. Morrison, in *Advances in Nuclear Physics*, edited by M. Baranger and E. Vogt (Plenum, New York, 1978), Vol. 9.
[21] S. Cohen and D. Kurath, Nucl. Phys. **73**, 1 (1965).
[22] E. Oset and D. Strottman, At. Data. Nucl. Data Tables **28**, 531 (1983).
[23] M. Mizoguchi and H. Toki, Nucl. Phys. **A513**, 685 (1990).
[24] E. Oset and D. Strottman, Phys. Lett. **84B**, 396 (1979).